# CORONAL TRANSIENTS NEAR SUNSPOT MAXIMUM

A. I. POLAND*, R. A. HOWARD, M. J. KOOMEN, D. J. MICHELS, and N. R. SHEELEY, Jr.

*E. O. Hulburt Center for Space Research, U. S. Naval Research Laboratory, Washington, D. C. 20375, U.S.A.*

(Received 12 February, 1980)

**Abstract.** The Naval Research Laboratory's most recent Earth-orbiting coronagraph, called Solwind, has been observing the Sun's outer corona ($2.6$–$10.0 R_\odot$) at 10-min intervals since March 28, 1979. These observations provide the first comprehensive view of coronal transients near the peak of a sunspot cycle. Six, well-defined transients in our quick-look data have masses ranging from $7 \times 10^{14}$ g to $2 \times 10^{16}$ g and outward speeds ranging from 150 km s$^{-1}$ to 900 km s$^{-1}$. These values are comparable to the ones that were obtained with the OSO-7 and Skylab observations during the declining phase of the last sunspot cycle. Although the amount of quick-look data is not sufficient to provide meaningful statistics, the coronal transients near sunspot maximum seem to occur with a greater frequency and a wider latitude range than the transients during the declining phase of the cycle. In both eras, there is a good, but imperfect, association between the occurrence of coronal transients and surface phenomena such as eruptive prominences and flares.

## 1. Introduction

The first comprehensive observations of coronal mass-ejection transients were obtained with the OSO-7 and Skylab coronagraphs during the declining phase of the last sunspot cycle (Howard *et al.*, 1975; Hildner, 1977; Munro *et al.*, 1979). The masses ranged from $1 \times 10^{15}$ g to $2.4 \times 10^{16}$ g and the outward speeds (in the plane of the sky) ranged from 100 km s$^{-1}$ to 960 km s$^{-1}$ (Hildner, 1977). The Skylab mass ejections occurred at relatively low latitudes with only 10% centered above 30° and none above 50° (Munro *et al.*, 1979). The shapes of these coronal mass ejections were distributed as follows: 33%-loops, 25%-clouds or blobs, and 42%-miscellaneous. During the Skylab mission (May 1973–February 1974), coronal mass ejections were observed on the average of once every three days, and of these observed transients only 44% were associated with definite or probable H$\alpha$ phenomena such as eruptive prominences or flares (Munro *et al.*, 1979).

The purpose of this paper is to present some observations of coronal mass ejections near the peak of the current sunspot cycle, and to compare these new observations with the ones obtained during the declining phase of the past cycle. In Section 2 we shall describe briefly the source and absolute calibration of the Solwind data. In Section 3 we shall characterize the mass ejections that we have seen in our preliminary sample of quick-look data near sunspot maximum. Finally, in Section 4 we will compare the characteristics of these transients with the mass ejections that were observed during the declining phase of the last cycle and consider briefly some of the implications of this comparison.

* On leave from the High Altitude Observatory, National Center for Atmospheric Research, Boulder, Colo. 80307, U.S.A. Now at Goddard Space Flight Center; Greenbelt, Md. 20771, U.S.A.

*Solar Physics* **69** (1981) 169–175. 0038-0938/81/0691-0169 $01.05.

## 2. The Source and Calibration of Coronal Images

Our study is based on coronal images that were obtained with the NRL white light coronagraph on the U.S. Department of Defense Space Test Program Satellite P78-1 (cf. Michels *et al.*, 1980a, b; Sheeley *et al.*, 1980a, b; Koomen *et al.*, 1980). This instrument is similar to the one described by Koomen *et al.* (1975) who observed the corona in 1971–1974 during the declining phase of the last sunspot cycle.

However, the new experiment has several advantages over the old one. First, its field of view is somewhat larger (2.6–10.0$R_\odot$ compared to 3.0–10.0$R_\odot$). Second, its net signal-to-noise ratio is greater (by an amount that we have not yet measured) due to the use of an improved vidicon detector. Third, its duty cycle is much greater (full-field images at 10-min intervals during the sunlit portion of each satellite orbit compared to one to four full-field images per day).

Our calibration technique was similar to the one that Koomen *et al.* (1975) used for the OSO-7 coronal images. In their technique, the telescope imaged a known, uniformly illuminated surface onto the focal plane detector. Then a series of calibrated, evaporated metal, neutral density filters was introduced and the responses of each of the $256 \times 256$ detector pixels was recorded. In this way the effects of telescope vignetting and vidicon sensitivity were combined into a single calibration.

The final absolute calibration was determined by matching the observed $K+F$ background coronal intensity (away from streamers) to the $K+F$ coronal intensity that Allen (1955) tabulated for sunspot maximum. In practice, we were able to match the $K+F$ intensities within a few percent. However, even such small uncertainties in the $K+F$ intensity introduce relatively large errors into the calibration of the $K$ coronal intensity because the $K$-component constitutes a relatively small portion of the total intensity at the radial distances in our 2.6–10.0$R_\odot$ field of view. Thus, when Allen's (1955) tabulated $F$ coronal intensities were subtracted from our calibrated $K+F$ measurements, the results differed from Allen's tabulated $K$ coronal intensities by as much as 40% in the range 2.6–6.0$R_\odot$.

Using the independent measurements of concentric and radial polarization contained in each image (cf. Koomen *et al.*, 1975), we were able to determine the location of transients with respect to the plane of the sky. As discussed by Koomen *et al.* (1975) and shown explicitly in Figure 1 for our observations, a scan along a given radial direction starting at the 2.6$R_\odot$ edge of the occulting disk gives the tangential component, $B_t$, of coronal intensity until the inner edge of the radial polarizer is encountered near 5$R_\odot$. Proceeding outward across the radial polarizer, the scan gives the radial component, $B_r$, of coronal intensity. Beyond approximately 6$R_\odot$, the scan gives the tangential component again. Thus, referring to Figure 1, at the midpoint of the radial polarizer one obtains $B_r$ directly (indicated by crosses in Figure 1) and $B_t$ indirectly by interpolating the tangential measurements across the radial polarizer (the dashed curve in Figure 1). Then, removing the $F$-component of

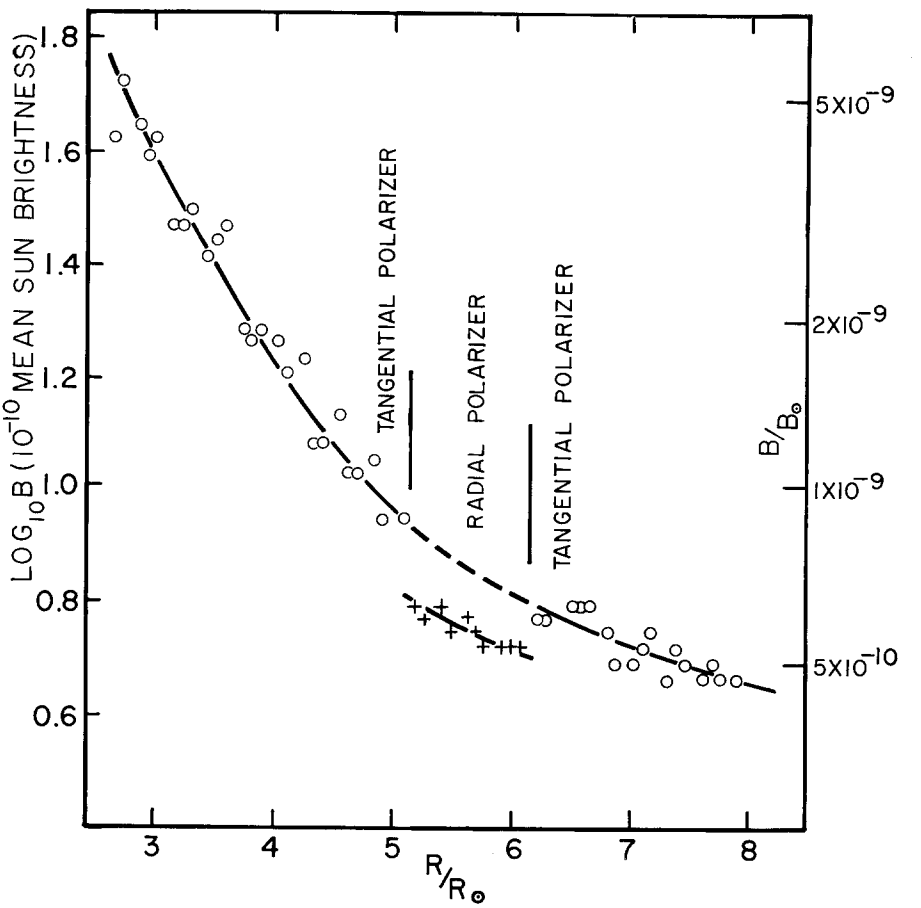


Fig. 1. Coronal intensity as a function of radial distance in the coronagraph's field of view. Open circles refer to the tangential component, $B_t$, and crosses refer to the radial component, $B_r$, of coronal intensity. The dashed line is an interpolation of the measurements of tangentially polarized radiation. $B_\odot$ is the mean solar brightness as defined by Allen (1955).

intensity from $B_t$ and $B_r$, one obtains the polarization of the $K$-component from the expression

$$\frac{(B_t-F)-(B_r-F)}{(B_t-F)+(B_r-F)}=\frac{B_t-B_r}{B_t+B_r-2F},$$

where $F$ is the intensity of the $F$-component. Finally, the angular location of the coronal structure relative to the plane of the sky is determined from the well-known relation between polarization, radial distance, and angle from the plane of the sky (cf. Poland and Munro, 1976). Of course, this interpolation is based on the assumption that the coronal feature extends across the radial polarizer in a direction that does not vary with its distance from the Sun.

## 3. Observations and Measurements

Although the extensive observational coverage of the Solwind satellite has undoubtedly produced a vast source of data on coronal mass ejections near sunspot maximum, to date we have received only a small sample (less than 5%) of quick-look data from the Air Force. In this section, we shall describe the characteristics of the six, well-defined coronal mass ejections of which we were aware at the time of this study. (We have found several more mass ejections since the preparation of this paper.)

Figure 2 shows each of the transients that we have studied. In each case solar north is up and east is to the left. Each photograph is a difference image obtained by subtracting a pre-transient image from the image in which the transient is in progress. The two events on May 8 and the event on September 27 seem to be shaped like loops. The August 14 transient may also fall in this category. The June 5 event has a poorly defined shape, but part of this confusion may result from obscuration by the occulter support which is located approximately 5° south of east. The May 7 transient had a 3-pronged shape.

Table I summarizes several characteristics of these transients. The outward speeds (in the plane of the sky) range from 150 km $s^{-1}$ to 900 km $s^{-1}$, and the increased

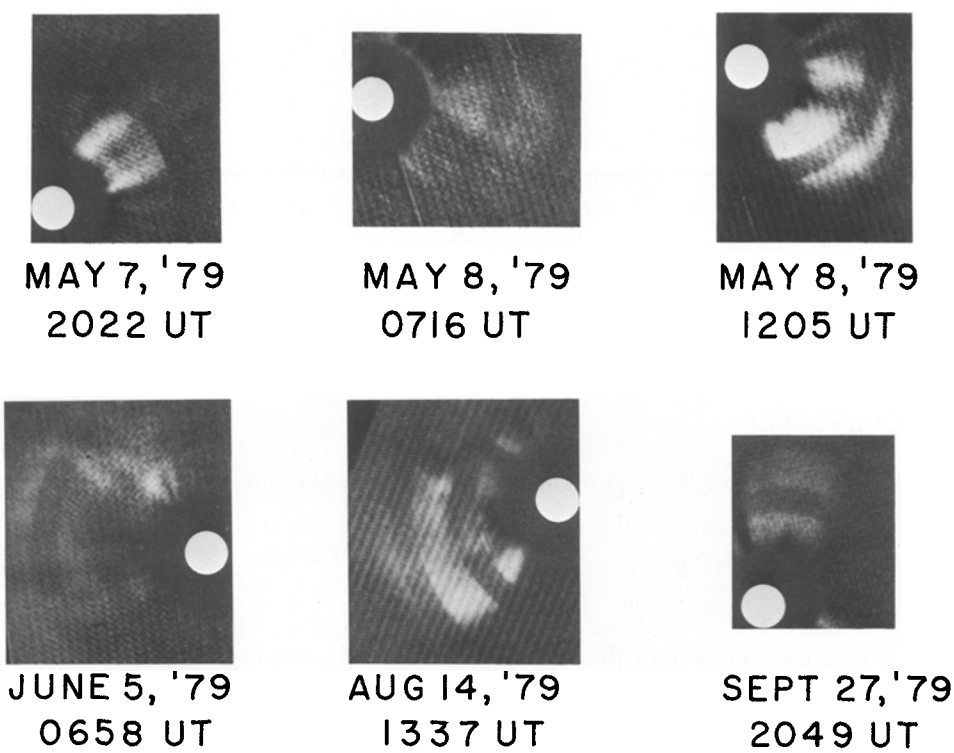


Fig. 2. The six transients that we have studied in our quick-look data. Each picture is a difference image obtained by subtracting a pre-transient image from the image at the indicated time. In each case, solar north is up and east is to the left. The white area indicates the size of the photospheric disk.

TABLE I

Transient characteristics

| Date | Mass ($10^{15}$ g) | Speed (km $s^{-1}$) | Limb position | Plane-of-sky angle | Association | Type |
|---|---|---|---|---|---|---|
| May 7 | 10 | 150 | 40 N–W | 0 | EPL | 3-prong |
| May 8 | 0.7 | 450 | 05 S–W | 0 | — | faint loop |
| May 8 | 8 | 500 | 35 S–W | 0 | EPL | loop |
| June 5 | 10 | 500 | 60 N–E* | 20 | metric burst | cloud |
| Aug. 14 | 20 | 900 | 20 S–E | 25 | flare | loop or cloud |
| Sept. 27 | 2.5 | – | 80 N–W | 20 | – | loop |

* Most of the observed emission occured between 40° and 60° N latitude, but some fainter emission may have been obscured by the occulter support whose center was located at approximately 5° S latitude on June 5.

masses in our 2.6–10.0$R_\odot$ field of view range from $7\times10^{14}$ g to $2\times10^{16}$ g. These transients are centered at latitudes that range from 5° to 80° from the Sun's equator. Two of these transients were associated with eruptive prominences (without reported H$\alpha$ flares) and one of the transients was associated with a typical large, long-duration X-ray flare complete with eruptive prominence and post-flare loops. Like similar events during the Skylab mission (Sheeley *et al.*, 1975), this August 14, 1979 transient had only a modest H$\alpha$ flare signature (1B or 1N). Nevertheless, it involved more mass and a higher speed than any other transient in Table I.

In Table I, the plane-of-the-sky angles are very uncertain. As we have mentioned earlier, they were derived from polarization measurements together with a knowledge of the way in which polarization depends on the plane-of-the-sky angle. For angles less than 25°, this function is so slowly-varying (cf. Poland and Munro, 1976) that one cannot easily distinguish plane-of-the-sky angles using polarization measurements. Thus, the angles listed in Table I indicate only that all of the transients lay close to the plane of the sky and that the last three events may have been slightly further from the plane than the first three.

In Table I, half of the transients were not associated with observed surface phenomena such as flares or eruptive prominences. In part, this imperfect association may result from data gaps in the NOAA patrol observations that we used to search for associations, and in part it may result from events that occurred on the backside of the Sun.

Although we have identified only six (now 10–15) mass ejections in our limited quick-look data, three (now four) of them occurred in a single, 24-hour interval when nearly continuous coverage was available (May 7–8). At this time, the sunspot number was approximately 150 (Lincoln, 1979) which is much greater than the average value of 50 that occurred during the OSO-7 and Skylab missions, but which is less than the values of 200–300 that have sometimes occurred during September–December 1979. Thus, our quick-look data are consistent with Hildner's (1977)

prediction that mass ejections might occur as frequently as three per day during sunspot maximum, but the final confirmation must await the receipt of the vast majority of our coronal observations.

## 4. Discussion

Based on our limited sample of quick-look data, it appears that the masses, speeds, shapes, and surface associations of coronal transients do not change significantly from the declining phase of the sunspot cycle to the peak of the cycle. We obtained masses in the range $7 \times 10^{14}$–$2 \times 10^{16}$ g with an average value of $8.5 \times 10^{15}$ g, whereas Hildner (1977) reported masses in the range $1 \times 10^{15}$–$2.4 \times 10^{16}$ g with an average of $6.2 \times 10^{15}$ g. Similarly, our range of speeds (150–900 km $s^{-1}$) does not differ appreciably from Hildner's (1977) range (100–960 km $s^{-1}$). During each era, approximately one-half of the observed mass ejections were associated with definite or probable H$\alpha$ phenomena such as flares or eruptive prominences. Significantly, in each era the fastest and most massive coronal ejection was associated with a large X-ray flare. During the declining phase of the cycle, 33% of the observed mass ejections were classified as loops wheras 50% of our six tabulated events can be classified as loops.

On the other hand, the latitude distribution and, apparently, the occurrence rate of coronal mass ejections change significantly from the declining phase of the sunspot cycle to the peak of the cycle. Although Munro *et al.* (1979) found that only 10% of the Skylab mass ejections were centered above 30° latitude (and none above 50°), three of our six events were centered above 35° and one of these transients was centered within approximately 10° of the north pole. Our sample of quick-look data is consistent with Hildner's (1977) prediction of three transients per day at sunspot maximum (compared to one per day during the Skylab mission). (Hildner's estimate of one transient per day during the Skylab mission was based on an observed average of one transient every three days and a duty cycle of approximately 30%.) Nevertheless, the sample is still too limited to provide a statistically significant confirmation.

These results have several implications. First, the coronal mass ejection mechanism is essentially unchanged throughout the sunspot cycle, but it probably occurs more frequently near sunspot maximum than near minimum. Second, the fact that coronal mass ejections have a broader latitude distribution than active regions suggests that either some of the ejections are not associated with active regions or some ejections are strongly non-radial or both. Indeed, one might suppose that near sunspot maximum some high latitude coronal mass ejections might be associated with the eruption of polar prominences (cf. Sheeley *et al.*, 1980c). Furthermore, if there were a tendency for the Sun's polar fields to deflect expelled coronal material toward the ecliptic near sunspot minimum (Hildner, 1977), then this tendency should be absent or even reversed near sunspot maximum when the polar fields are weak and the large scale fields are centered at lower latitudes. Third, the net mass flux from coronal transients is greater near sunspot maximum than near sunspot minimum,

especially at latitudes poleward of 35°. When we have received the remainder of our data, it will be interesting to measure the net mass flux from coronal transients and to compare it with the in-ecliptic mass flux in the solar wind as Hildner (1977) did for the Skylab era.

## Acknowledgements

The effort to orbit a small coronagraph capable of nearly continuous solar monitoring has received substantial assistance from several sources. The NASA Office of Solar Physics provided spare coronagraph and solar pointing flight hardware from its OSO-7 program, and furnished the ground station support that has allowed quick access to the Solwind data. The Department of Defense Space Test Program was responsible for the P78-1 vehicle and for integration, launch, and operations support. The Office of Naval Research provided financial support. At NRL, D. Roberts, F. Harlow, R. Chaimson, and R. Seal provided the technical and engineering support that was essential to make this project a success.

## References

Allen, C. W.: 1955, *Astrophysical Quantities*, The Athlone Press, Univ. of London, London, p. 143.

Hildner, E.: 1977, in M. A. Shea, D. F. Smart and S. T. Wu (eds.), *Study of Travelling Interplanetary Phenomena*, D. Reidel Publ. Co., Dordrecht, Holland, p. 6.

Howard, R. A., Koomen, M. J., Michels, D. J., Tousey, R., Detwiler, C. R., Roberts, D. E., Seal, R. T., Whitney, J. D., Hansen, R. T., Hansen, S. F., Garcia, C. J., and Yasukawa, E.: 1975, Report UAG-48, *World Data Center A for Solar-Terrestrial Physics*, NOAA, Boulder, Colorado.

Koomen, M. J., Detwiler, C. R., Brueckner, G. E., Cooper, H. W., and Tousey, R.: 1975, *Appl. Opt.* **14**, 743.

Koomen, M. J., Sheeley, Jr., N. R. Michels, D. J., and Howard, R. A.: 1980, *Sky Telesc.* **60**, 102.

Lincoln, J. V.: 1979, *EOS* **60**, 1027.

Michels, D. J., Howard, R. A., Koomen, M. J., and Sheeley, Jr., N. R.: 1980a, in M. R. Kundu and T. E. Gergely (eds.), 'Radio Physics of the Sun', *IAU Symp.* **86**, 439.

Michels, D. J., Howard, R. A., Koomen, M. J., Sheeley, Jr., N. R., and Rompolt, B.: 1980b, in M. Dryer and E Tandberg-Hanssen (eds.), 'Solar and Interplanetary Dynamics', *IAU Symp.* **91**, 387.

Munro, R. H., Gosling, J. T., Hildner, E., MacQueen, R. M., Poland, A. I., and Ross, C. L.: 1979, *Solar Phys.* **61**, 201.

Poland, A. I. and Munro, R. H.: 1976, *Astrophys. J.* **209**, 927.

Sheeley, Jr., N. R., Bohlin, J. D., Brueckner, G. E., Purcell, J. D., Scherrer, V. E., Tousey, R., Smith, Jr., J. B., Speich, D. M., Tandberg-Hanssen, E., Wilson, R. M., de Loach, A. C., Hoover, R. B., and McGuire, J. P.: 1975, *Solar Phys.* **45**, 377.

Sheeley, Jr., N. R., Howard, R. A., Michels, D. J., and Koomen, M. J.: 1980a, in M. Dryer and E. Tandberg-Hanssen (eds.), 'Solar and Interplanetary Dynamics', *IAU Symp.* **91**, 55.

Sheeley, Jr., N. R., Michels, D. J., Howard, R. A., and Koomen, M. J.: 1980b, *Astrophys. J. Letters* **237**, L99.

Sheeley, Jr., N. R., Howard, R. A., Koomen, M. J., Michels, D. J., and Poland, A. I.: 1980c, *Astrophys. J. Letters* **238**, L161.

Van de Hulst, H. C.: 1953, in G. P. Kuiper (ed.), *The Sun*, University of Chicago Press, Chicago, Illinois, p. 264.